

Wideband estimation of the drive torque of a wind turbine using LiDAR measurements, blade element momentum theory and Kalman filtering

N. Ell¹, M. Stubbe¹, D. Turschner¹ and H.-P. Beck¹

¹ Institute for Electrical Power Engineering and Energy Systems
Power Mechatronics
Clausthal University of Technology
Leibnizstrasse 28, 38678 Clausthal, Germany
Phone/Fax number: +49 5323 723821, e-mail: nikola.ell@tu-clausthal.de

Abstract In this paper a method to estimate the drive torques from Light Detection and Ranging (LiDAR) measurements is proposed. Knowledge of these values brings many advantages for turbine control and especially active damping of mechanical oscillations.

Primarily a simplified method to calculate the aerodynamic torque from wind speed measurements of a nacelle based LiDAR-system will be presented which bases on blade element momentum theory (BEM). Comparisons of results of the original and a simplified computation method show small deviations in the relevant working range of a wind turbine. Additionally a Kalman Filter is used to estimate the drive torques of the wind turbine.

The method is tested in simulation using a model of a doubly fed induction generator (DFIG) wind turbine including a gearbox. Simulation results show good performance of the estimation.

Key words

Wind energy, LiDAR, blade element momentum theory, Kalman Filter, estimation.

1. Introduction

Wind power plants have to be absolutely reliable. Drive train damages are one major reason for turbine breakdowns, as all mechanical components are highly stressed by oscillations, which are induced by the wind load and several kinds of special events.

A number of concepts to enhance the durability of the drive elements have been proposed in recent years. Besides optimization of design and engineering of the mechanical turbine components themselves as proposed in [1], it is a viable method to modify the control algorithms of the turbine, either of the pitch control [2] or of the generator controller [3]-[8].

These control algorithms could be optimized if more drive train measurements are available. As measuring this value is a very complex and costly task, using estimation algorithms is a possible alternative. Different methods for load

estimation have been proposed using a variety of mechanical sensor signals and anemometer wind speed measurements [9]-[11].

Light Detection and Ranging (LiDAR) is a technology for remote sensing using laser light. By evaluating the reflected light the distance or speed of objects can be measured. Among others one possible application is measuring the speed of aerosol particles in the atmosphere to determine the wind speed [12],[13].

A nacelle based LiDAR-System offers new possibilities of wind turbine control, especially in terms of active damping of drive train oscillations. Different control approaches using feedforward and feedback control for pitch [14]-[17] or generator control [18] have been proposed, some of which include observation of the turbine

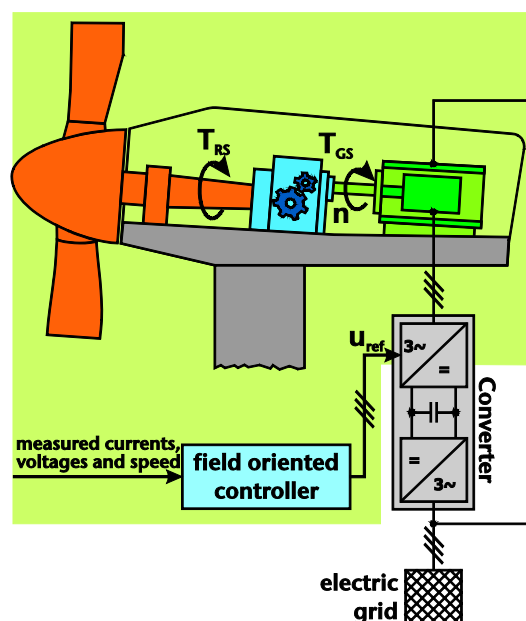


Fig. 1: Schematic diagram of a wind turbine with DFIG and gearbox. The colored parts have been modeled (illustration based on [7]).

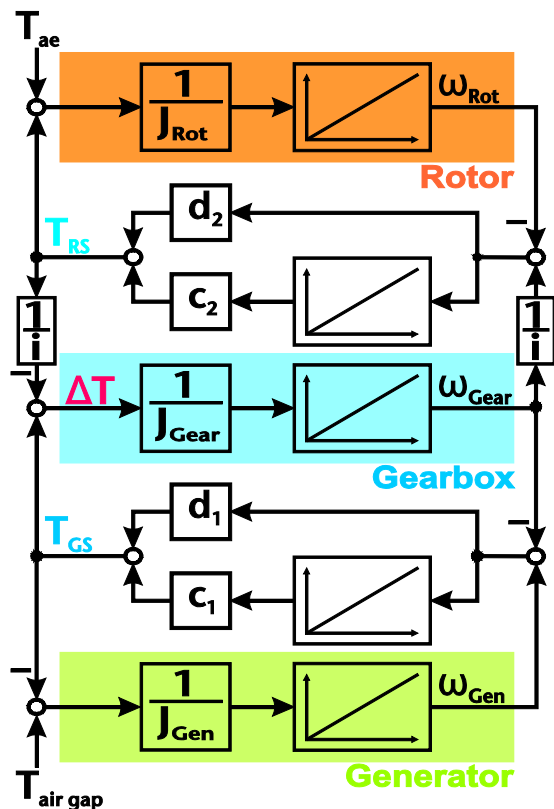


Fig. 2: Block diagram of a three mass oscillator (illustration based on [7]).

system using LiDAR measurements [17],[18]. Nevertheless all of them do not use LiDAR to determine high frequency drive train oscillations.

This paper presents a new method to estimate the drive torque of a wind turbine using wind speed measurements of a nacelle based LiDAR-System and a Kalman Filter. The Kalman Filter uses the aerodynamic torque T_{ae} , which is induced by the turbine rotor, as an input value. Furthermore a simplified method to compute T_{ae} online using blade element momentum theory (BEM) is proposed.

Simulations will be carried out using a simulation model of a doubly fed induction generator (DFIG) wind turbine including a gearbox.

2. System under consideration and modelling

In this paper we will take a variable speed doubly fed induction generator (DFIG) wind turbine with a planetary gearbox as an example. This type of turbine is commonly

used nowadays. A scheme of a wind power plant of the type examined can be found in Figure 1. In general it is possible to use the new concepts on any kind of turbine later on. Simulations are carried out using Matlab/Simulink.

The DFIG is modelled using the equations described in [19]. Its stator is directly connected to the electric grid and its rotor is connected to a converter. The machine is controlled via the converter by a commonly accepted field oriented control method as described in [20].

The mechanical drive train is represented as a three-mass-oscillator. In the following we will refer to the torque on the high speed shaft of the gearbox (generator side) as T_{GS} and to the torque on the low speed shaft (rotor side) as T_{RS} . The gear ratio is given by i . Looking at the block diagram of a three-mass-oscillator (c.f. Figure 2), it is obvious, that the mechanical components and especially the gearbox is loaded by the differential torque ΔT . It can be calculated by

$$\Delta T = T_{GS} - \frac{T_{RS}}{i} \quad (1)$$

A time varying wind field has been computed using TurbSim by NREL [21]. It outputs a wind speed matrix in the rotor plane for each time step, which is used as an input for the rotor model. It calculates the aerodynamic torque T_{ae} using blade element momentum theory (BEM). A description of the equations can be found in section 4.

3. Measuring wind speed using LiDAR

Light Detection and Ranging (LiDAR) is a remote sensing technology similar to Radar, but using Laser light instead of micro waves.

Laser light is emitted in direction of an object and the reflected light gathered and evaluated. Using a Doppler LiDAR system the speed of objects can be measured by analyzing the Doppler shift of the backscattered light. The speed of aerosol particles in the atmosphere can be used to determine the wind speed. A detailed description of LiDAR systems can be found in [12],[13].

In this paper we assume that the considered wind turbine has a nacelle based Doppler-LiDAR-System installed, that allows measuring higher frequency wind speed oscillations ($f > 10\text{Hz}$). At the moment there is no such system available on the market, but considering ongoing research it will be available in the future [22]-[24].

We assume we have the output of this measurement device available as a matrix of wind speed in the rotor plane. Furthermore we assume that the torque on the high speed shaft of the wind turbine T_{GS} is measured.

4. Calculation of the aerodynamic torque T_{ae}

The rotor of a wind turbine transforms the kinetic energy of the wind in a mechanical torque on the drive train. Finally electrical power can be generated using a generator.

In this section a method will be described to calculate the aerodynamic torque T_{ae} on the main shaft of the wind turbine from the arising wind velocity v .

The computation is done using blade element momentum theory (BEM) which considers the local forces on infinitesimally small blade elements at each radius r . A de-

tailed description of the method can be found in [25]-[27].

A **z** bladed wind turbine is considered. Each rotor blade is described by its blade width $h(r)$ starting at radius r_0 , the rotor blade radius R_R and the lift coefficient c_A , which is considered constant for the whole blade. The width of one blade element for the BEM computation is $\Delta r(r)$.

The angular frequency of the rotor is described by ω_{rot} and the air density by ρ .

Concluding the following equations can be derived:

$$T_{ae} = E_1 \sum_{i=1}^{\frac{R_R - r_0}{\Delta r}} E_2 E_3 \quad (2)$$

while:

$$E_1 = \frac{\rho}{3} c_A \quad (3)$$

$$E_2 = r_i h(r_i) \Delta r(r_i) \quad (4)$$

$$E_3 = v \sqrt{\frac{4}{9} v(r, t)^2 + \omega_{rot}^2(t) r_i^2} \quad (5)$$

5. Simplified method to calculate the aerodynamic torque T_{ae}

Looking at equations (2) - (5) one can see, that the three sub-functions E_1 , E_2 and E_3 can be distinguished by their variable dependencies on wind velocity v , angular frequency of the rotor ω_{rot} and radius r .

The first sub-function E_1 consists solely of constant factors ($E_1 = \text{const}$). It is neither dependent on time t nor blade radius r . Therefore it can be calculated once for the whole turbine and all time.

The second sub-function E_2 depends on the blade radius r , but not on time t ($E_2 = f(r)$). The rotor geometry does not change during turbine operation. Thus E_2 can be obtained once for each blade element and all time.

The third sub-function E_3 is time t and radius r depending. Thus it has to be computed in each time step Δt ($E_3 = f(v, \omega_{rot}, r)$) using the measured values v and ω_{rot} .

This last sub-function E_3 solely determines the complexity of the online computation of the aerodynamic torque T_{ae} . The other sub-functions can be pre-calculated and do not influence the computation time.

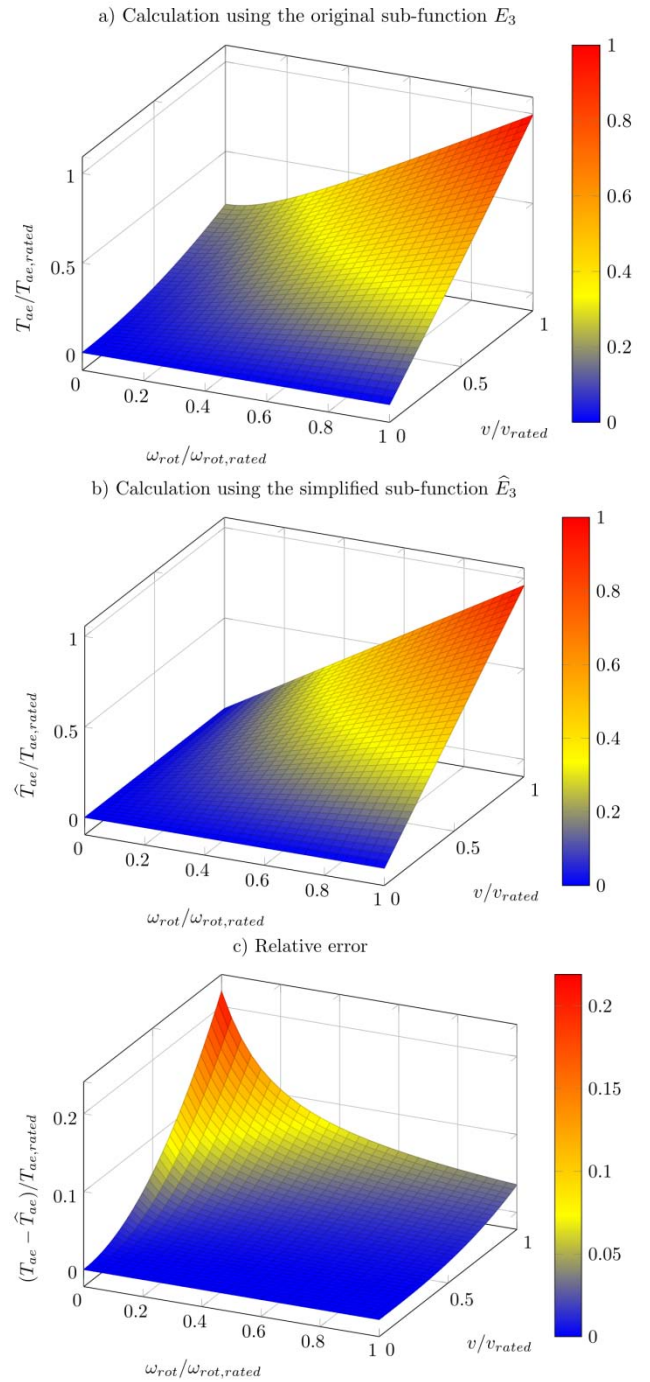


Fig. 3: Aerodynamic torque T_{ae} plotted against the angular frequency ω_{rot} and the wind velocity v . You can see the values computed using the original sub-function E_3 (a), the simplified sub-function \hat{E}_3 (b) and the relative error (c).

We aim to find a simplified computation method \hat{E}_3 to replace E_3 , which calculates good results in the relevant working range of a wind turbine.

In the following low angular frequencies ω_{rot} and wind velocities v are neglected, as there is very little energy capture in this working range of the wind turbine. Than it holds for $\omega_{rot} r \gg 0$:

$$\omega_{rot} r \gg \sqrt{\frac{4}{9} v} \quad (6)$$

Considering this observation we calculate a simplified sub-function \hat{E}_3 as follows:

$$E_3 = v \sqrt{\frac{4}{9}v^2 + \omega_{rot}^2 r^2} \approx v \omega_{rot} r = \hat{E}_3 \quad (7)$$

Figure 3 shows the aerodynamic torque T_{ae} plotted against the angular frequency ω_{rot} and the wind velocity v . It has been calculated using data of a common wind turbine. For the sake of simplicity a constant wind velocity v on the whole blade is assumed.

You can see the aerodynamic torque T_{ae} computed using the original sub-function E_3 (a), the simplified sub-function \hat{E}_3 (b) and the relative error of \hat{E}_3 (c). As expected the biggest deviations can be found for low angular frequencies ω_{rot} , which are neglected.

Thus Figure 3 shows clearly that the simplified computation method using \hat{E}_3 gives good results as deviations are very low in the relevant working range of a wind turbine.

6. Observation of T_{RS} and ΔT using a Kalman filter

The Kalman Filter is an algorithm to estimate unknown system states x using measurements observed over time y which include measurement uncertainties (e.g. noise). In addition a state space model of the system and the system input values u are known.

The algorithm works in a two-step cycle. In the prediction step a new estimation for the system states \hat{x} is calculated. In the next step this estimation is corrected using the measurements y . Detailed information about this algorithm can be found in [28]-[30].

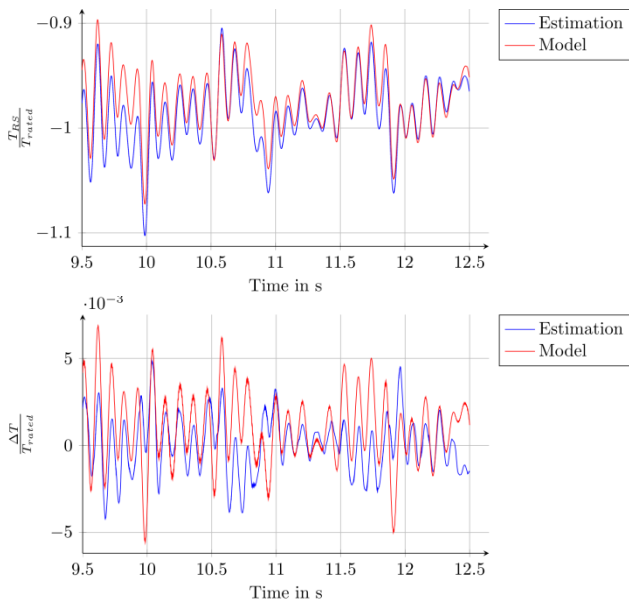


Fig. 4: Simulation results of the torque on the low-speed shaft T_{RS} (top) and the differential torque ΔT (bottom) over time. The values of the estimation (blue) and the wind turbine model (red) show a similar trend.

In this paper we will estimate the states of the mechanical system of the wind turbine, that is all speeds ($\omega_{gen}, \omega_{gear}, \omega_{rot}$) and the resulting shaft torsions ($\varphi_{gen} - \varphi_{gear}$ and $\frac{\varphi_{gear}}{i} - \varphi_{rot}$). We consider the state space model of the mechanical system as three-mass oscillator.

The generator speed ω_{gen} and the torque on the high speed shaft T_{GS} have to be measured and result in y . The vector of input values u includes the aerodynamic torque T_{ae} which has been calculated using the simplified computation method described in section 5 and the air gap torque of the generator $T_{air\ gap}$, which can be calculated in a flux model.

The torques T_{GS} and T_{RS} arise from the estimated states and the known values of the mechanical spring rigidity c and damping d .

$$T_{GS} = d_1(\varphi_{gen} - \varphi_{gear}) + c_1(\omega_{gen} - \omega_{gear}) \quad (8)$$

$$T_{RS} = d_2\left(\frac{\varphi_{gear}}{i} - \varphi_{rot}\right) + c_2\left(\frac{\omega_{gear}}{i} - \omega_{rot}\right) \quad (9)$$

Afterwards the differential torque ΔT can be calculated using equation (1)

7. Simulation results

Simulations have been carried out using Matlab/Simulink and the model described in section 2.

The simulation results can be found in Figure 4. The values of estimation and model show a similar trend. Especially the high frequency oscillations are well reproduced by the estimation as nearly all peaks are shown.

The values of the torque on the low-speed shaft T_{RS} show less deviations of estimation and model than the differential torque ΔT . This can be explained by the influence of the measured torque T_{GS} and the much smaller range of the values.

Thus the proposed estimation method using the simplified calculation of the aerodynamic torque T_{ae} and Kalman filtering works very well. The estimated values of the torque on the low-speed shaft T_{RS} (above) and the differential torque ΔT will be a good basis for control design and damping of drive train oscillations.

8. Conclusion

A new simplified method to calculate the aerodynamic torque T_{ae} from wind speed measurements of a nacelle based LiDAR-System using blade element momentum theory (BEM) has been presented. Comparisons of results of the original and the simplified computation methods show small deviations in the relevant working range of a wind turbine.

Furthermore a Kalman Filter has been used to estimate the torque on the low-speed shaft T_{RS} and the differential torque ΔT of the wind turbine. Simulations show good estimation results.

Knowledge of these values of the drive train brings many advantages for turbine control and especially active damping of mechanical oscillations. Measuring this value is a very complex and costly task. Therefore estimation can be a good alternative.

To make the described methods work, further improvements concerning LiDAR-systems are mandatory. Further research has to result in industrial solutions for nacelle based measurement infrastructure. Higher sampling rates are needed as well as a severe cost reduction of the systems. In addition systems to measure the torque on the high speed shaft T_{GS} have to be further developed and brought to the market.

In future research it is planned to combine the proposed algorithms with control algorithms for active damping of oscillations in the drive train of a wind power plant as proposed in [7],[8].

To prove the new concepts in a more realistic environment by measurements they will be tested on a 37kW test rig (c.f. Figure 5) that emulates the behaviour of the drive train of a DFIG wind power plant.

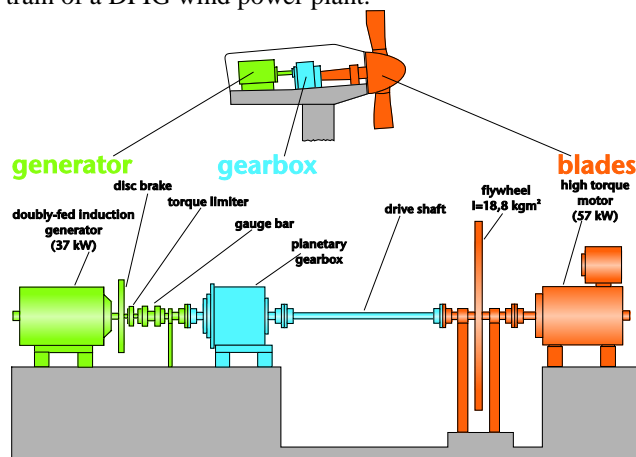


Fig. 5: Schema of the 37kW DFIG wind power plant test rig (illustration based on [7]).

References

- [1] H. Long, J. Wu, and A. Firth, "Improving gearbox design and analysis for offshore wind turbines," In: *Applied Mechanics and Materials*, vol. 86, pp. 309-312.
- [2] G.A. Parker and C.D. Johnson, "Use of Reduced-Order Observers for Feedback Control in Large Wind Turbines May Reduce Fatigue Damage from Excitement of Flexible Modes," In: *Proceedings of 42nd South Eastern Symposium on System Theory 2010*, Tyler (USA).
- [3] H. Geng, D. Xu, B. Wu and G. Yang, "Active Damping for Torsional Vibrations in PMSG based WECS," In: *Proceedings of 25th Applied Power Electronics Conference (APEC) 2010*, Palm Springs.
- [4] G. Mandic, F. Oyague and E. Muljadi, "Mechanical Stress Reduction in Variable Speed Wind Turbine Drivetrains," In: *Proceedings of 3rd IEEE Energy Conversion Congress und Exposition (ECCE) 2011*, Phoenix.
- [5] R. Muszynski and J. Deskur, "Damping of Torsional Vibrations in High-Dynamic Industrial Drives," In: *IEEE Transactions on Industrial Electronics*, vol 57, pp. 544-552.
- [6] G. Mandic, A. Nasiri, E. Muljadi and F. Oyague, "Active Torque Control for Gearbox Load Reduction in a Variable-Speed Wind Turbine," In: *IEEE Transactions on Industry Applications*, vol. 48, no. 6, pp. 2424-2432.
- [7] N. Ell, D. Turschner and H.-P. Beck, "Active Damping of Oscillations on the Drive Train of a Wind Power Plant Using Field Oriented Control," In: *Proceedings of DEWEK - 11th German Wind Energy Conference 2012*.
- [8] N. Ell, D. Turschner and H.-P. Beck, "Active Damping of Oscillations on the Drive Train of a Synchronous Generator Wind Turbine using Field Oriented Control and the MILD Controller Concept," In: *Proceedings of 1st. Global Virtual Conference (GV-CONF) 2013*, Goce Delchev University Macedonia & THOMSON Ltd. Slovakia.
- [9] M. Hau, *Promising Load Estimation Methodologies for Wind Turbine Components*, Deliverable 5.2, Project UpWind.
- [10] B. Jasiewicz, *Online Estimation of Mechanical Loads for Wind Turbines*, Deliverable 5.3, Project UpWind.
- [11] S. Kanev and T. van Engelen, "Wind Turbine Extreme Gust Control," In: *Wind Energy*, vol. 13, pp. 18-35.
- [12] T. Fukuchi and T. Shiina, *Industrial Applications of Laser Remote Sensing*, Bentham Science Publishers (2012).
- [13] C. Weitkamp, *Lidar - Range-Resolved Optical Remote Sensing of the Atmosphere*. Springer Series in Optical Sciences, volume 102, Springer, New York (2005).
- [14] F. Dunne, L. Pao, A. Wright B. Jonkman and N. Kelley, "Combining Standard Feedback Controllers with Feedforward Blade Pitch Control for Load Mitigation in Wind Turbines," In: *Proceedings of 48th AIAA Aerospace Sciences Meeting Including the New Horizons Forum and Aerospace Exposition 2010*.
- [15] F. Dunne, L. Y. Pao, A. D. Wright, B. Jonkman, N. Kelley, and E. Simley, "Adding Feedforward Blade Pitch Control for Load Mitigation in Wind Turbines: Non-Causal Series Expansion, Preview Control, and Optimized FIR Filter Methods," In: *Proceedings of AIAA Aerospace Sciences Meeting 2011*, Orlando, Florida.
- [16] D. Schlipf, S. Schuler, P. Grau, F. Allgöwer and M. Kühn, "Look-Ahead Cyclic Pitch Control using LIDAR," In: *Proceedings of Torque 2010: The Science of Making Torque from Wind*, Heraklion, Crete.
- [17] E. Bossanyi, B. Savini, M. Iribas, M. Hau, B. Fischer, D. Schlipf, T. van Engelen, M. Rossetti and C.E. Carcangiu, "Advanced controller research for multi-MW wind turbines in the UPWIND project," In: *Wind Energy*, vol 15: pp. 119-145.
- [18] D. Schlipf, D.J. Schlipf and M. Kühn, "Nonlinear model predictive control of wind turbines using LIDAR," In: *Wind Energy*, vol. 16: pp.1107-1129.
- [19] D. Schröder, *Elektrische Antriebe 1: Grundlagen*, 4th. Edition, Springer, Dordrecht (2009) (German).
- [20] S. Heier, *Windkraftanlagen: Systemauslegung, Netzintegration und Regelung*, 4th. edition, B.G.Teubner Verlag, Wiesbaden (2005) (German).

- [21] N. Kelley, N. and B. Jonkman, Overview of the TurbSim Stochastic Inflow Turbulence Simulator: Version 1.21 , Technical Report, National Renewable Energy Laboratory, NREL/TP-500-41137, Golden, Colorado (2007).
- [22] Y. Han, X. Dou, D. Sun; H. Xia and, Z. Shu, “Analysis on wind retrieval methods for Rayleigh Doppler lidar,” In: Optical Engineering vol. 53, no. 6, 2014, pp. 061607.1–061607.8.
- [23] G.J. Koch, J.Y. Beyon, L.J. Cowen, M.J. Kavaya and M.S. Grant, “Three-dimensional wind profiling of off-shore wind energy areas with airborne Doppler lidar,” In: Journal of Applied Remote Sensing, vol. 8, no. 1, pp. 083662.1–083662.11.
- [24] E. Simley, L.Y. Pao, R. Frehlich, B. Jonkman and N. Kelley, “Analysis of light detection and ranging wind speed measurements for wind turbine control,” In: Wind Energy, vol 17, pp. 413–433.
- [25] R. Gasch and J. Tvele, Windkraftanlagen: Grundlagen, Entwurf, Planung und Betrieb, 4th Edition, Vieweg+Teubner Verlag, Wiesbaden (2005) (German).
- [26] M. O. L. Hansen, Aerodynamics of Wind Turbines, 2nd Edition, Earthscan, London and Sterling, VA (2008).
- [27] J.-P. Moll, Windenergie in Theorie und Praxis: Grundlagen u. Einsatz, Verlag C.F. Müller, Karlsruhe (1978) (German).
- [28] R.E. Kalman, „A New Approach to Linear Filtering and Prediction Problems,“ In: Journal of Basic Engineering vol. 82, no. 1, pp.35-45.
- [29] P.S. Maybeck, Stochastic Models, Estimation and Control, volume 1, Academic Press, New York (1979).
- [30] B. Teixeira, „Kalman Quickie [ask the experts]“. In: Control Systems, IEEE, vol. 30, no. 2, pp. 17–18.